Sensitivity of entanglement decay of quantum-dot spin qubits to the external magnetic field

Paweł Mazurek,[1,2] Katarzyna Roszak,[3,*] Ravindra W. Chhajlany,[4,5] and Paweł Horodecki[1,6]
[1]*National Quantum Information Centre of Gdańsk, 81-824 Sopot, Poland*
[2]*Institute for Theoretical Physics and Astrophysics, University of Gdańsk, 80-952 Gdańsk, Poland*
[3]*Institute of Physics, Wrocław University of Technology, 50-370 Wrocław, Poland*
[4]*Faculty of Physics, Adam Mickiewicz University, 61-614 Poznań, Poland*
[5]*ICFO-Institut de Ciéncies Fotóniques, Mediterranean Technology Park, E-08860 Castelldefels, Barcelona, Spain*
[6]*Faculty of Applied Physics and Mathematics, Gdańsk University of Technology, 80-952 Gdańsk, Poland*
(Received 8 May 2013; revised manuscript received 4 May 2014; published 17 June 2014)

We study the decay of entanglement of quantum-dot electron-spin qubits under hyperfine-interaction-mediated decoherence. We show that two-qubit entanglement of a single entangled initial state may exhibit decay characteristic of two disentanglement regimes in a single sample, when the external magnetic field is changed. The transition is manifested by the suppression of time-dependent entanglement oscillations which are superimposed on the slowly varying entanglement decay related to phase decoherence which results in oscillatory behavior of entanglement sudden death time as a function of the magnetic field. This unique behavior allows us to propose the double-quantum-dot two-electron spin Bell state as a promising candidate for precise measurements of the magnetic field.

DOI: 10.1103/PhysRevA.89.062318 PACS number(s): 03.67.Mn, 73.21.La, 03.65.Ud, 03.65.Yz

I. INTRODUCTION

Systems of electron spins confined in quantum dots (QDs) have received much theoretical (see Refs. [1–3] for review) and experimental (see Refs. [4–6] for review) interest since the initial proposal for spin-based quantum computing [7]. This has resulted in the development of a range of effective techniques for the initialization, manipulation, and readout of the spin state in two main trends: one involving electrical (or magnetic) manipulation of lateral QDs [8–10] and the other involving optical manipulation of self-assembled QDs [11–13]. Both have proven successful in the generation of high-fidelity initial states, also entangled, but the coherent evolution of spin states and the manipulation thereof suffer from the destructive effects of the hyperfine interaction between the electron spin and the spins of the nuclei of the QD atoms. Hence, the current experiments focus mostly on few-spin qubits [14,15] which are more robust against decoherence, or on involved schemes for the minimization of decoherence effects [16–18]. The proficiency attained in the experiments has been very recently demonstrated in Ref. [19], where quantum state tomography of two initially entangled singlet-triplet qubits has been performed.

The central idea of this paper is to propose, based on the high level of the experimental techniques used to study electron spin states in QDs, a scheme for sensing an external parameter (the magnetic field) by harnessing the entanglement present in a two-qubit system and the inbuilt decoherence processes. The idea is outside of traditional methods in quantum metrology, since it relies on decoherence, while metrology requires a high degree of quantum coherence. Since it has been shown that the quantum enhancement in metrology reduces to the shot-noise limit due to quantum noise for the most popular scheme [20], investigations regarding other types of quantum estimation methods gain relevance. Here, it is vital that the qubits be electron spins confined in QDs with a nonzero nuclear spin of the environment, because this leads to the specific system-environment interaction and results in a characteristic disentanglement process, which, as we have found, strongly and counterintuitively depends on the magnetic field.

The study of spin entanglement [21] decay in a two-electron two-QD system has up to date been limited to a number of complex, yet solvable scenarios [22–24]. The complexity accounts for the nontrivial behavior of the reported evolution of entanglement. Hence, in Refs. [22] and [23] the uniform coupling ("box") model is extended to account for the exchange interaction between electron spins for a small number of nuclei in the common nuclear bath limit (with low bath polarization) and separate nuclear baths limit (with high bath polarization and large exchange interaction), respectively. Reference [24] utilizes the "box" model with a simplified thermal spin bath state to introduce a scheme for multipartite entanglement generation mediated by interaction with a nuclear bath. An exception is Ref. [25], where the evolution of entanglement of noninteracting spin qubits is studied, but the decoherence model considered is phenomenological and leads to a type of decoherence different than what has been found in other literature [2,3]. The importance of Ref. [25] lies in its attempt to quantify multipartite entanglement under a feasibly realistic evolution of the qubit states.

This paper is organized as follows. In the following section, the system of QD spin qubits, the Hamiltonian, and the possible single-dot evolutions are described. Section III describes the evolution of entanglement in a double-quantum-dot (DQD) system and contains the main results of this article. Section IV discusses the potential application of the system for magnetometry and Section V concludes the paper.

II. THE SYSTEM AND THE HAMILTONIAN

We study the evolution of entanglement of two noninteracting electron spin qubits confined in two well-separated lateral GaAs QDs. The qubits interact via the hyperfine coupling

*Present address: Department of Condensed Matter Physics, Faculty of Mathematics and Physics, Charles University, 12116 Prague, Czech Republic.

with separate nuclear spin reservoirs, which are taken in the high-temperature thermalized state to which the baths relax quickly at experimentally accessible temperatures [26]. Hence, we can use the "box" model for the whole range of magnetic field values [27,28], because entanglement decay takes place on time scales shorter than the "box" model limit of applicability, $t < N/A$, where N denotes the number of nuclei and $A = \sum_k A_k$ is the sum of coupling constants between the electron and the nuclei.

We show that the nature of entanglement decay changes substantially when the transition to the high-magnetic-field limit is made, $g\mu_B B \gg A$. To this end, we study the entanglement decay of an initial Bell state, for which sudden death (SD) of entanglement [29,30] (complete disentanglement while the loss of coherence is still only partial) is not possible under pure dephasing processes [31]. At high magnetic fields decoherence is restricted to pure dephasing and, since entanglement is proportional to the coherence, it decays following the appropriate exponential function. Contrarily, at low magnetic fields the evolution involves a redistribution of the spin-up and spin-down occupation. This leads to entanglement oscillations, which are superimposed on the slowly varying entanglement decay from phase decoherence, and to entanglement SD. Hence, the same system realizes qualitatively different disentanglement scenarios in different magnetic field regimes for the same initial entangled state.

The system can be described by a separable Hamiltonian, $H = H_1 \otimes \mathbb{I}_2 + \mathbb{I}_1 \otimes H_2$, where the individual QD subsystems are described by Hamiltonians of the form (the magnetic field is applied in the z direction)

$$H_i = -g\mu_B \hat{S}_i^z B + \sum_k A_{k,i} \hat{S}_i^z \hat{I}_{k,i}^z + \frac{1}{2} \sum_k A_{k,i} (\hat{S}_i^+ \hat{I}_{k,i}^- + \hat{S}_i^- \hat{I}_{k,i}^+), \quad (1)$$

with the index $i = 1,2$ distinguishing the two dots. The first term in Eq. (1) is the electron Zeeman splitting, where g is the effective electron g factor, μ_B is the Bohr magneton, $\hat{S}_i^z$ is the component of the electron spin parallel to the magnetic field, and B denotes the applied magnetic field. The last two terms describe the hyperfine interaction between the spin of an electron and the spins of the surrounding QD nuclei. The diagonal (second) term is also known as the Overhauser term and leads to pure dephasing, while the last term, known as the "flip-flop" term, is responsible for both dephasing and leveling out of the electron spin occupations. Here, $\hat{\mathbf{I}}_{k,i}$ are spin operators of the individual nuclei (discriminated by the index k) in dot i. $\hat{I}_{k,i}^z$ is the z component, while $\hat{I}_{k,i}^{\pm} = \hat{I}_{k,i}^x \pm i\hat{I}_{k,i}^y$ are the nuclear spin raising and lowering operators. Analogously, $\hat{S}_i^{\pm} = \hat{S}_i^x \pm i\hat{S}_i^y$ are the raising and lowering operators for the electron spin. The coupling constants of the hyperfine interaction depend on the species of the nuclei and on its location with respect to the electron wave function,

$$A_{k,i} = A_{k,i}^0 v_0 |\Psi_i(\mathbf{r}_{k,i})|^2, \quad (2)$$

where $A_{k,i}^0 = \frac{2}{3}\mu_0 \gamma_e \gamma_{k,i}$ are the coupling constants of a given nuclear species found at site k of dot i, with μ_0 denoting the vacuum magnetic permeability, γ_e and $\gamma_{k,i}$ being the electron and nuclear gyromagnetic ratios, respectively, while v_0 is the unit cell volume of the QD crystal, $\Psi_i(\mathbf{r})$ is the wave function of the electron located in dot i, and $\mathbf{r}_{k,i}$ is the position of the kth nucleus in dot i.

We have omitted the nuclear Zeeman term and the dipolar interaction between nuclei in the Hamiltonian (1), the first because nuclear Zeeman energies of gallium and arsenic are very small and the resulting energy splittings are of the order of tens of neV (corresponding to less than a mK) for each tesla of magnetic field applied to the system. The nearest-neighbor dipolar coupling constants between nuclei are even smaller and are of the order of 0.1 neV. Hence, at typical experimental temperatures both nuclear terms in the Hamiltonian are much smaller than $k_B T$ [3,27].

For the same reason the nuclear baths can be described by infinite-temperature, fully mixed density matrices [3,26] unless the state of the nuclear environment is especially experimentally prepared. While a polarized environment strongly changes the resulting dynamics and leads to an increase of the electron spin coherence time [32,33], the preparation of such an environment is demanding experimentally [34,35] and the currently attainable levels of polarization are under 70% [36]. The study of polarized environments is beyond the scope of this paper, where we wish to describe spin disentanglement in the simplest and most common scenario. Hence, we limit the study to initial states, for which the density matrix of the two-qubit subsystem and the two nuclear reservoirs is in the product state $\varrho(0) = \rho_{\mathrm{DQD}}(0) \otimes R_1(0) \otimes R_2(0)$, where $\rho_{\mathrm{DQD}}(0)$ is the initial state of the two confined electron spins, while the nuclear baths R_i are initially fully mixed.

We use parameters corresponding to two identical lateral GaAs QDs, but the results are qualitatively valid for any dot type, as long as they can be treated as noninteracting (are sufficiently far away from each other). Electron wave-function envelopes, which are necessary to find the coupling constants of the hyperfine interaction, Eq. (2), are modeled by anisotropic Gaussians with the extension $l_\perp = 20$ nm in the xy plane and $l_z = 2$ nm along the z direction, which is the direction of the applied magnetic field. The number of crystal unit cells considered within each dot is $N_1 = N_2 \approx 1.5 \times 10^6$.

All isotopes naturally found in GaAs carry spin $I = 3/2$ and the nuclear-species-dependent coefficients $A_{i,k}^0$ are equal to $A_{^{69}\mathrm{Ga}} = 36$ μeV, $A_{^{71}\mathrm{Ga}} = 46$ μeV, and $A_{^{75}\mathrm{As}} = 43$ μeV [37,38]. The relative abundances of the gallium isotopes are 60.4% for ^{69}Ga and 39.6% for ^{71}Ga; this together with the fact that there is one gallium and one arsenic atom in the GaAs unit cell gives the average hyperfine coupling constant $A = 83$ μeV. The g factor is equal to $g = -0.44$ [39]; hence, the Zeeman electron spin splitting is equal to 25.5 μeV per tesla of magnetic field.

The parameters are used to find single-QD evolutions in the high-magnetic-field limit, $g\mu_B B \gg A$, for which the "flip-flop" term may be completely neglected. The condition is fulfilled for magnetic fields greater than about 3.25 T. The Hamiltonian is then diagonal and it is possible to find the evolution for a realistic distribution of coupling constants while taking into account the large number of nuclei. The resulting dynamics is limited to pure dephasing which is further independent of the magnetic field (and local unitary oscillations that do not disturb entanglement) for the initial high-temperature environment. As predicted [27], the decay

of a single spin is proportional to $\exp(-t^2/T_2^{*2})$, with a characteristic constant $T_2^* = \sqrt{\frac{6}{I(I+1)}}\sqrt{N}/A$. $\sqrt{N}/A \approx 10$ ns according to the parameters used and the $T_2^* = 12.36$ ns extracted from the calculation corroborates this.

To quantify single-dot evolution at lower magnetic fields, we use the "box" model which is valid on short time scales when the high-temperature nuclear bath density matrix is used and at high magnetic fields converges with the approach above. The upper limit of short-time-scale behavior is approximated by N/A [38], the value of which is 1.2×10^4 ns for the parameters used and exceeds the disentanglement times by 3 orders of magnitude. In the box model, the hyperfine coupling terms are assumed constant $A_k = \alpha = A/N$, which allows for exact diagonalization of the Hamiltonian (1) as outlined in the Appendix. Furthermore, box model evolutions involving a large number of nuclei can be successfully simulated with reasonably small numbers of nuclei, since few-body coherent effects disappear already in the case of 10 spins 3/2 and for 50 spins large-number-of-nuclei evolutions are reproduced (see the Appendix for details).

The single-QD evolution depends strongly on the magnetic field. At very low magnetic fields, QD occupations are partially leveled out due to the interaction with the environment and phase decoherence closely resembles the decay of the occupation difference. The effect of the environment on the occupations is diminished with a growing magnetic field, while coherence damping remains strong, although it starts to resemble exponential decay. When the limit of high magnetic fields is reached, the interaction with nuclear spins cannot disturb the occupations, and the pure dephasing process follows a Gaussian decay proportional to $\exp(-t^2/T_2^{*2})$.

III. EVOLUTION OF ENTANGLEMENT

The study of entanglement evolution requires a two-qubit entanglement measure which can be calculated from the system state. One such measure, for which an explicit formula is available, is the concurrence [40,41], which is closely related to the entanglement of formation, defined as the ensemble average of the von Neumann entropy minimized over all ensemble preparations of the state [42,43]. The concurrence for bipartite entanglement is given by $C(\rho_{\mathrm{DQD}}) = \max\{0, \lambda_1 - \lambda_2 - \lambda_3 - \lambda_4\}$, where λ_i are the square roots of the eigenvalues of the matrix $\rho_{\mathrm{DQD}}(\sigma_y \otimes \sigma_y)\rho^*_{\mathrm{DQD}}(\sigma_y \otimes \sigma_y)$. Here, ρ_{DQD} is the two-qubit density matrix, ρ^*_{DQD} is its complex conjugate, and σ_y is the appropriate Pauli matrix.

We study the entanglement evolution of the initial maximally entangled Bell states, $|\Psi^{\pm}\rangle = 1/\sqrt{2}(|1\rangle \pm |2\rangle)$ and $|\Phi^{\pm}\rangle = 1/\sqrt{2}(|0\rangle \pm |3\rangle)$, where the states in the single-QD basis are equal to $|0\rangle = |\uparrow\uparrow\rangle$, $|1\rangle = |\uparrow\downarrow\rangle$, $|2\rangle = |\downarrow\uparrow\rangle$, and $|3\rangle = |\downarrow\downarrow\rangle$. The evolution of the coherences for these initial states is limited to the single off-diagonal element of the density matrix which is initially nonzero, while the other coherences remain zero at all times. Contrarily, all four occupations are influenced (except for the high-magnetic-field limit where the decoherence is a pure dephasing process) by the interaction. Hence, the DQD density matrix is simplified and the concurrence is always given by

$$C(\rho_{\mathrm{DQD}}) = 2\max\{0, |\rho_{ij}| - \sqrt{\rho_{kk}\rho_{ll}}\}, \qquad (3)$$

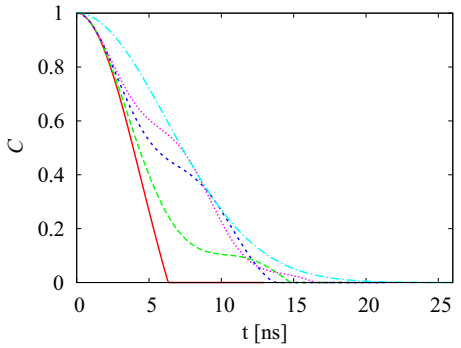

FIG. 1. (Color online) Time evolution of entanglement for different magnetic field values: $B = 0$ mT, solid red line; $B = 11$ mT, long-dashed green line; $B = 16.5$ mT, dashed blue line; $B = 20$ mT, dotted pink line; and $B = 1000$ mT, dashed-dotted blue line (high-magnetic-field limit).

where i, j are equal to 1,2 or 0,3 depending on the initial state, and $k \neq l$, $k \neq i$, $k \neq j$, $l \neq i$, and $l \neq j$. It is evident from Eq. (3) that SD of entanglement will occur when $|\rho_{ij}| < \sqrt{\rho_{kk}\rho_{ll}}$, so it is expected in the low-magnetic-field regime when the QD occupations are disturbed, while it will not occur for high-magnetic-field pure dephasing. This is due to a transition made between the phase and amplitude damping decoherence channels present at low magnetic fields and the purely phase damping channel at high magnetic fields. To the best of our knowledge, such an effect has not been shown either theoretically or experimentally in any solid state system. A number of papers showing the appearance of two regimes of entanglement decay have been reported previously, but it was either (i) the result of changing the initial state [30,31,44,45] or (ii) the result of more fundamental changes made to the studied system that resulted in the change of the decoherence channel [46,47], such as modifying the system-environment interaction by changing structural parameters of the qubits [48,49] or changing the type of the environment [50]. Furthermore, because the qubits interact with separate environments at high-temperature thermal equilibrium, the evolution of entanglement is the same for all four Bell states.

Figure 1 shows entanglement decay for different magnetic field values. The zero-magnetic-field curve (red solid) limits all higher-magnetic-field curves from below and ends in SD. The high-magnetic-field curve (dashed-dotted blue line) provides the upper limit for the concurrence at a given time and undergoes exponential decay. In between, the curves corresponding to small magnetic fields display a more complex entanglement evolution. According to Eq. (3), the visible oscillations are due to the interplay of the dephasing process and the shifts in the occupations. The number of oscillations increases with the increase of the magnetic field, while they become less pronounced, because the high magnetic field inhibits occupation changes. The suppression of the oscillations is a manifestation of the transition between the two types of disentanglement.

It is due to those oscillations that the SD times are not a monotonous function of the magnetic field, as seen in Fig. 2. At low magnetic fields, a strong oscillatory behavior is evident, starting from around 10 mT. For higher magnetic fields, ρ_{ij}

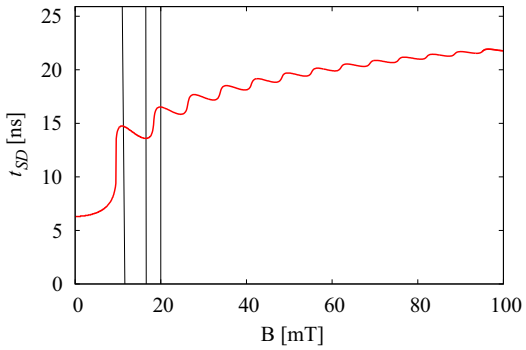

FIG. 2. (Color online) Entanglement SD time t_{SD} as a function of the magnetic field. The vertical lines mark the magnetic field values corresponding to the long-dashed green, dashed blue, and dotted pink lines in Fig. 1. Between 5 and 10 mT the SD time is a good indicator of the magnetic field value.

decays as $\exp[-\sigma^2 t^2]$, while $\rho_{kk} = \rho_{ll}$, which initially equals 0, oscillates with the amplitude proportional to $\frac{\sigma^2}{B^2}$, where $\sigma^2 \sim A^2/N$. The equality between the two, responsible for the SD of entanglement, gives an estimated $t_{\mathrm{SD}} \sim \sqrt{2 \ln \frac{B}{\sigma}}/\sigma$ valid for high magnetic fields.

IV. MAGNETOMETRY

For any fixed time, the considered dynamics is a tensor product of two quantum channels (completely positive trace preserving maps) which are both bistochastic—they preserve the maximally mixed state. The proof of this statement is straightforward, namely, consider a single-qubit subsystem in a maximally mixed state coupled by an arbitrary unitary interaction to the maximally mixed environment state. Since the product of identities is the identity operator on the composed (qubit + environment) system and is invariant under any unitary operation, the final state of the two subsystems remains the same product of maximally mixed states. In particular, the maximally mixed state of the qubit subsystem is preserved. The argument applies to each of the QDs separately. It follows that any two-qubit state with maximally mixed subsystems will retain the property during the evolution. A system with maximally mixed subsystems has to have Bell diagonal qubit states [51], and starting from the Bell diagonal state guarantees Bell diagonality for the whole evolution. It is known that, when a Bell diagonal state becomes separable in the course of its evolution, the entanglement fidelity F becomes $1/2$ [51]. We start from a single Bell state $|\Psi_0\rangle$ (a trivial Bell diagonal state) and the maximal eigenvalue corresponds to the projection onto that state. Monitoring the difference of that eigenvalue and $1/2$, i.e., $W(t) = \frac{1}{2} - F = \frac{1}{2} - \langle\Psi_0|\rho(t)|\Psi_0\rangle$ (which is a specific entanglement witness), we may identify the moment of entanglement SD exactly. This means that the zero point time t^* of $W(t)$ is just the SD time, $t^* = t_{\mathrm{SD}}$, and as such has the same dependence on the magnetic field as shown in Fig. 2. Quite remarkably, W as an entanglement witness is directly measurable. In fact, the initialization of a singlet state (one of the Bell states for spin-up and spin-down qubits) and the measurement of its fidelity has been demonstrated in Ref. [10]. Reference [52] contains recent results demonstrating the initialization of a triple-dot spin state with better fidelity, whereas in Ref. [53] very good singlet initialization in silicon-based DQDs is demonstrated. By measuring the fidelity we can get the exact estimate of the magnetic field whenever it corresponds to the initial monotonic regime of the sudden death of entanglement function of Fig. 2. In the regions close to the steep parts of this function, the above value is quite sensitive to the field B and can be considered as a threshold sensor of the magnetic field.

V. CONCLUSION

We have studied decay of QD spin-qubit Bell state entanglement under decoherence processes mediated by hyperfine interaction. We have shown that varying the magnetic field leads to a transition between substantially different entanglement decay processes, which is manifested by the suppression of oscillations in the time evolution of entanglement. Furthermore, at low magnetic fields, the evolution of entanglement displays counterintuitive oscillatory behavior which results in a nonmonotonic dependence of the SD time on the magnetic field. The characteristic behavior is an outcome of the interplay of the decay of the system coherence with the decoherence-induced redistribution of the DQD spin occupations and can serve as the basis for constructing a threshold magnetic field sensor utilizing quantum entanglement and quantum decoherence. Remarkably, a similar model has been applied to the radical pair mechanism of magnetoreception which is expected to explain the nature of magnetic orientation for some species of birds [54–57], yielding qualitatively similar SD behavior [54]. Our model has the chance of being the first entanglement-based magnetometry prototype with a solid state realization for which the quantum noise is the driving mechanism for the measurement.

ACKNOWLEDGMENTS

The authors thank Bill Coish and Łukasz Cywiski for helpful discussions. The authors acknowledge support from the National Science Centre Project 2011/01/B/ST2/05459. This work was supported by the TEAM programme of the Foundation for Polish Science cofinanced from the European Regional Development Fund (K.R.). P.M. was supported by the Foundation for Polish Science International Ph.D. Projects Programme cofinanced by the EU European Regional Development Fund. R.W.C acknowledges funding from the Polish Ministry of Science and Higher Education through a Mobility Plus fellowship.

APPENDIX: THE "BOX MODEL"

In the box model, the hyperfine coupling terms are assumed to be constant $A_k = \alpha = A/N$, which allows for the exact diagonalization of the single-dot Hamiltonian [Eq. (2) in the main article] as outlined below.

First, it is now possible to rewrite the single-dot Hamiltonian in terms of the components of the total nuclear spin operator $\hat{K}_i = \sum_k \hat{I}_{k,i}$. Furthermore, it is convenient to use the eigenstates of the total nuclear spin and its z component as the nuclear environment basis states, $\{|K,m\rangle\}$, described by the

spin quantum numbers K and m, $m = -K, -K+1, \ldots, K$, and fulfilling the relations $\hat{K}_i^2|Km\rangle = \hbar^2 K(K+1)|Km\rangle$ and $\hat{K}_i^z|Km\rangle = \hbar m|Km\rangle$. Note, that the Hamiltonian [Eq. (2) in the main article] acting on any state $|\sigma; K,m\rangle$, where $\sigma = \uparrow, \downarrow$ denotes the electron spin, cannot change the nuclear quantum number K and conserves the z component of the total spin of the combined electron and nuclear spin system. Hence, the Hamiltonian can be represented in an easily diagonalizable 2×2 block form, where each block links the states $|\uparrow; K,m\rangle$ and $|\downarrow; K,m+1\rangle$, which form a closed subspace for every K and $m \in [-K, K-1]$. The form of these 2×2 blocks is given by

$$\begin{bmatrix} E_m & M_{K,m} \\ M_{K,m} & -E_{m+1} \end{bmatrix},$$

where the energies are given by $E_m = \hbar/2(\Omega + \alpha m)$, with the Zeeman frequency $\Omega = -g\mu_B B/\hbar$, and the transitions are governed by $M_{K,m} = \hbar\alpha/2\sqrt{K(K+1) - m(m+1)}$. The eigenvectors are then of the following forms:

$$|+; K,m\rangle = \cos\theta_{K,m}|\uparrow; K,m\rangle + \sin\theta_{K,m}|\downarrow; K,m+1\rangle,$$
$$|-; K,m\rangle = -\sin\theta_{K,m}|\uparrow; K,m\rangle + \cos\theta_{K,m}|\downarrow; K,m+1\rangle,$$

with

$$\sin\theta_{K,m} = \frac{M_{K,m}}{(E^+_{K,m} + E_{m+1})^2 + M^2_{K,m}}, \tag{A1}$$

and with corresponding eigenenergies given by

$$E^{\pm}_{K,m} = \frac{-\hbar\alpha/2 \pm \sqrt{(E_m + E_{m+1})^2 + 4M^2_{K,m}}}{2}. \tag{A2}$$

Furthermore, the $|\uparrow; K,K\rangle$ and $|\downarrow; K, -K\rangle$ states are eigenvectors of the Hamiltonian. Hence, the evolution of any combined state of the electron and nuclear spins can be found.

The high-temperature nuclear-spin density matrix, rewritten in the $\{|K,m\rangle\}$ basis, takes the diagonal form

$$R(0) = \sum_{K,m} P_{K,m}|K,m\rangle\langle K,m|, \tag{A3}$$

where $P_{K,m}$ are coefficients describing the multiplicity of the occupation of each state and satisfy the relation $\sum_{K,m} P_{K,m} = 1$. For nuclei with spin s they are given by [58]

$$P_{K,m} \sim \sum_i (-1)^i \binom{N}{i} \binom{(s+1)N - (2s+1)i - K - 2}{N-2}, \tag{A4}$$

where $i \in [0, N]$ is an integer. For spin-1/2 systems the formula simplifies to

$$P_{K,m} \sim \frac{N!(2K+1)}{(\frac{1}{2}N - K)!(\frac{1}{2}N + K + 1)!}. \tag{A5}$$

The evolution of the QD density matrix can be found by tracing out the environmental degrees of freedom and assuming a product initial state $\rho(0) = \rho_{\mathrm{QD}}(0) \otimes R(0)$, with the initial QD density matrix denoted by $\rho_{\mathrm{QD}}(0)$ and the nuclear-spin density matrix $R(0)$ given by Eq. (A3). It is described by

$$\begin{aligned}\rho_{\mathrm{QD}}(t) = {} & |\uparrow\rangle\langle\uparrow|\{\rho_{\uparrow\uparrow}(0)X(t) + \rho_{\downarrow\downarrow}(0)[1 - X'(t)]\} \\ & + |\downarrow\rangle\langle\downarrow|\{\rho_{\uparrow\uparrow}(0)[1 - X(t)] + \rho_{\downarrow\downarrow}(0)X'(t)\} \\ & + |\uparrow\rangle\langle\downarrow|[\rho_{\uparrow\downarrow}(0)Y(t)] + \mathrm{H.c.}\end{aligned} \tag{A6}$$

Here, $X(t) = \sum_{K,m} P_{K,m}|X_{K,m}(t)|^2$, $X'(t) = \sum_{K,m} P_{K,m}|X_{K,m-1}(t)|^2$, and $Y(t) = \sum_{K,m} P_{K,m} X_{K,m}(t)X_{K,m-1}(t)$, with

$$X_{K,m}(t) = \cos^2\theta_{K,m} e^{-\frac{i}{\hbar}\phi_{K,m}t} + \sin^2\theta_{K,m} e^{\frac{i}{\hbar}\phi_{K,m}t}.$$

The phase coefficients are equal to

$$\phi_{K,m} = \frac{\hbar\sqrt{\Omega^2 + \Omega\alpha(2m+1) + \frac{\alpha^2}{4} + \alpha^2 K(K+1)}}{2},$$

and the mixing angles $\theta_{K,m}$ are given by Eq. (A1). Note that for a large number of nuclei N the time-dependent functions $X(t)$ and $X'(t)$ coincide, and the evolution of the diagonal terms of the density matrix is described by

$$\Delta\rho(t) = \Delta\rho(0)[2X(t) - 1], \tag{A7}$$

with $\Delta\rho(t) = \rho_{\uparrow\uparrow}(t) - \rho_{\downarrow\downarrow}(t)$.

Even though the box model is exactly solvable as reproduced above, finding the actual QD evolution when the environment is in the high-temperature equilibrium state becomes numerically challenging very quickly with the growing number of nuclei N, due to the involved summation over K and m, and is practically impossible for realistically large values of N. The difficulty of the task also grows rapidly with higher spins of the nuclear species taken into account. Figures 3 and 4 serve to demonstrate that box model evolutions involving a large number of nuclei can be successfully simulated with reasonably small numbers of nuclei, since the few-body coherent effects disappear already in the case of 10 spins 3/2 and for 50 spins a large number of nuclei evolutions are reproduced. The necessary condition to achieve convergence is that $A/\sqrt{N}$ remains constant. This requirement

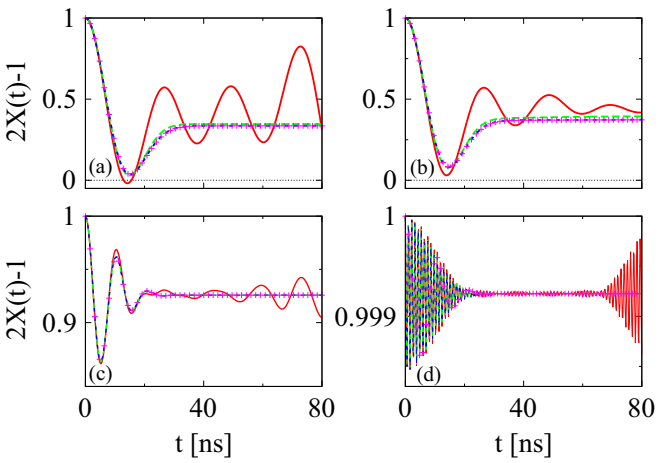

FIG. 3. (Color online) Box model evolution of the difference of single-QD occupations $\Delta\rho(t)/\Delta\rho(0)$ (see text) for $B = 0$ mT (a), 1.5 mT (b), 15 mT (c), and 150 mT (d). Different curves correspond to different numbers of spin-3/2 environment nuclei, $N = 2$ (red solid line), 10 (green dashed line), and 50 (blue dotted line). Points denote the evolution fitted with 300 nuclei with spin-1/2.

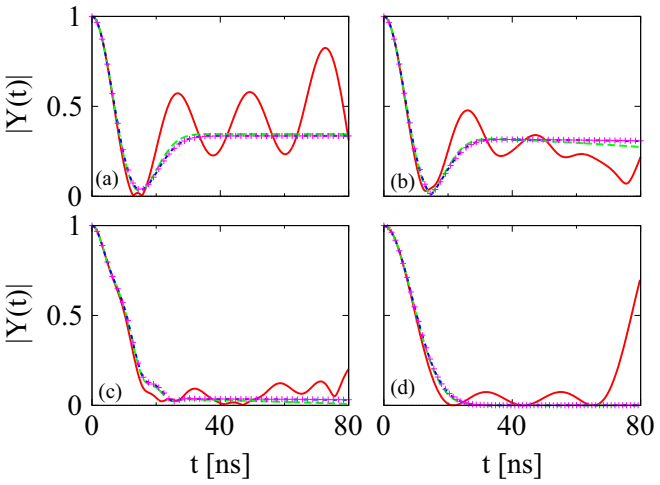

FIG. 4. (Color online) Box model evolution of the amplitude of single-QD coherence $\rho_{\uparrow\downarrow}(t)/\rho_{\uparrow\downarrow}(0)$ (see text) for $B = 0$ mT (a), 1.5 mT (b), 15 mT (c), and 150 mT (d). Different curves correspond to different numbers of spin-3/2 environment nuclei, $N = 2$ (red solid line), 10 (green dashed line), and 50 (blue dotted line). Points denote the evolution fitted with 300 nuclei with spin-1/2.

stems from the semiclassical approximation [27] result giving the characteristic decay time $T_2^* \approx \sqrt{\frac{6}{I(I+1)}}\sqrt{N}/A$, where I is the nuclear spin.

Figure 3 contains plots of the function $1 - 2X(t)$ which determines the evolution of the QD occupations for large N [see Eq. (A7)] for four different magnetic field values as a function of time. We have found that the function $X'(t)$ converges for similar values of N as the function $X(t)$; hence no additional plots are necessary. Analogously, the plots of the evolution of the amplitude of the off-diagonal terms $|Y(t)| = |\rho_{\uparrow\downarrow}(t)/\rho_{\uparrow\downarrow}(0)|$ are shown in Fig. 4 for the same values of the magnetic field. In each plot, there are three curves corresponding to spin-3/2 nuclei, with $N = 2$, 10, and 50. We have also found the evolutions for $N = 500$ and $N = 2000$, but the resulting curves are indistinguishable from the 50 nuclei curves on relevant time scales and, hence, have not been included in the plots. As can be seen, the effects resulting from a limited number of spins are strong only for very small N. They manifest themselves as additional oscillations of the two nuclei occupation curves and echolike characteristics resulting from the alignment of the few nuclear spins at certain time intervals.

The type of evolution manifested by the single-QD system depends strongly on the value of the magnetic field. At very low magnetic fields, the occupations of the QD are redistributed due to the interaction with the environment [see Figs. 3(a) and 3(b)]. In this regime, the phase decoherence closely resembles the decay of the occupation difference [Figs. 4(a) and 4(b)]. The effect of the environment on the occupations is diminished with the growing magnetic field [Figs. 3(c) and 3(d)], while coherence damping remains strong, although it starts to resemble exponential decay [Figs. 4(c) and 4(d)]. When the limit of high magnetic fields is reached, the interaction with nuclear spins cannot disturb the QD occupations, and the pure dephasing process follows a Gaussian decay proportional to $\exp(-t^2/T_2^{*2})$.

Analysis of spin-1/2 environments further simplifies the generation of QD system evolutions for a given number of nuclei. To quantify the applicability of such an approximation, points have been added to the plots of Figs. 3 and 4, which denote the evolutions found by modeling the spin-3/2 environment with a spin-1/2 nuclei for $N = 300$. The large number of nuclei is necessary to achieve convergence for spins 1/2. The fitting required a scaling of the constants α by $\sqrt{\frac{I_{3/2}(I_{3/2}+1)}{I_{1/2}(I_{1/2}+1)}} = \sqrt{5}$, with $I_{3/2} = \frac{3}{2}$ and $I_{1/2} = \frac{1}{2}$, deduced from semiclassical approximation. The resulting evolutions are qualitatively and quantitatively reproduced very well and the transitions between different types of decoherence with a growing magnetic field are the same as in the case of the spin-3/2 environment. Unfortunately, the large number of environment atoms required diminishes any computational advantages, which would be gained by using nuclei with smaller spins.

[1] W. A. Coish and J. Baugh, Phys. Stat. Sol. B **246**, 2203 (2009).
[2] W. A. Coish, J. Fischer, and D. Loss, Phys. Rev. B **81**, 165315 (2010).
[3] Ł. Cywiński, Acta Phys. Pol. A **119**, 576 (2011).
[4] R. Hanson *et al.*, Rev. Mod. Phys. **79**, 1217 (2007).
[5] R. Hanson and D. D. Awschalom, Nature (London) **453**, 1043 (2008).
[6] A. J. Ramsay, Semicond. Sci. Technol. **25**, 103001 (2010).
[7] D. Loss and D. P. DiVincenzo, Phys. Rev. A **57**, 120 (1998).
[8] J. M. Elzerman *et al.*, Nature (London) **430**, 431 (2004).
[9] R. Hanson, L. H. Williams van Beveren, I. T. Vink, J. M. Elzerman, W. J. M. Naber, F. H. L. Koppens, L. P. Kouwenhoven, and L. M. K. Vandersypen, Phys. Rev. Lett. **94**, 196802 (2005).
[10] J. R. Petta *et al.*, Science **309**, 2180 (2005).
[11] M. Kroutvar *et al.*, Nature (London) **432**, 81 (2004).
[12] S. Spatzek, A. Greilich, S. E. Economou, S. Varwig, A. Schwan, D. R. Yakovlev, D. Reuter, A. D. Wieck, T. L. Reinecke, and M. Bayer, Phys. Rev. Lett. **107**, 137402 (2011).
[13] D. Kim *et al.*, Nat. Phys. **7**, 223 (2011).
[14] E. A. Laird, J. M. Taylor, D. P. DiVincenzo, C. M. Marcus, M. P. Hanson, and A. C. Gossard, Phys. Rev. B **82**, 075403 (2010).
[15] N. S. Lai *et al.*, Sci. Rep. **1**, 110 (2011).
[16] A. Greilich *et al.*, Science **317**, 1896 (2007).
[17] C. Barthel, J. Medford, H. Bluhm, A. Yacoby, C. M. Marcus, M. P. Hanson, and A. C. Gossard, Phys. Rev. B **85**, 035306 (2012).
[18] J. Medford, Ł. Cywiński, C. Barthel, C. M. Marcus, M. P. Hanson, and A. C. Gossard, Phys. Rev. Lett. **108**, 086802 (2012).
[19] M. D. Shulman *et al.*, Science **336**, 202 (2012).

[20] R. Demkowicz-Dobrzański, J. Kołodyński, and M. Guţă, Nat. Commun. **3**, 1063 (2012).
[21] R. Horodecki, P. Horodecki, M. Horodecki, and K. Horodecki, Rev. Mod. Phys. **81**, 865 (2009).
[22] B. Erbe and J. Schliemann, Phys. Rev. B **81**, 235324 (2010).
[23] B. Erbe and J. Schliemann, Phys. Rev. B **85**, 155127 (2012).
[24] H. Christ, J. I. Cirac, and G. Giedke, Phys. Rev. B **78**, 125314 (2008).
[25] F. Bodoky, O. Gühne, and M. Blaauboer, J. Phys.: Condens. Matter **21**, 395602 (2009).
[26] A. Abragam, *The Principles of Nuclear Magnetism* (Oxford University Press, New York, 1983).
[27] I. A. Merkulov, A. L. Efros, and M. Rosen, Phys. Rev. B **65**, 205309 (2002).
[28] E. Barnes, Ł. Cywiński, and S. Das Sarma, Phys. Rev. B **84**, 155315 (2011).
[29] K. Życzkowski, P. Horodecki, M. Horodecki, and R. Horodecki, Phys. Rev. A **65**, 012101 (2001).
[30] T. Yu and J. H. Eberly, Phys. Rev. Lett. **93**, 140404 (2004).
[31] K. Roszak and P. Machnikowski, Phys. Rev. A **73**, 022313 (2006).
[32] W. A. Coish and D. Loss, Phys. Rev. B **70**, 195340 (2004).
[33] W. Zhang, V. V. Dobrovitski, K. A. Al-Hassanieh, E. Dagotto, and B. N. Harmon, Phys. Rev. B **74**, 205313 (2006).
[34] E. A. Chekhovich, M. N. Makhonin, K. V. Kavokin, A. B. Krysa, M. S. Skolnick, and A. I. Tartakovskii, Phys. Rev. Lett. **104**, 066804 (2010).
[35] G. Petersen, E. A. Hoffmann, D. Schuh, W. Wegscheider, G. Giedke, and S. Ludwig, Phys. Rev. Lett. **110**, 177602 (2013).
[36] B. Urbaszek *et al.*, Rev. Mod. Phys. **85**, 79 (2013).
[37] R.-B. Liu, W. Yao, and L. J. Sham, New J. Phys. **9**, 226 (2007).
[38] Ł. Cywiński, W. M. Witzel, and S. Das Sarma, Phys. Rev. B **79**, 245314 (2009).
[39] S. Adachi, J. Appl. Phys. **58**, R1 (1985).
[40] S. Hill and W. K. Wootters, Phys. Rev. Lett. **78**, 5022 (1997).
[41] W. K. Wootters, Phys. Rev. Lett. **80**, 2245 (1998).
[42] C. H. Bennett, G. Brassard, S. Popescu, B. Schumacher, J. A. Smolin, and W. K. Wootters, Phys. Rev. Lett. **76**, 722 (1996).
[43] C. H. Bennett, H. J. Bernstein, S. Popescu, and B. Schumacher, Phys. Rev. A **53**, 2046 (1996).
[44] J. Dajka, M. Mierzejewski, and J. Łuczka, Phys. Rev. A **77**, 042316 (2008).
[45] X.-F. Qian and J. Eberly, Phys. Lett. A **376**, 2931 (2012).
[46] J.-H. Huang and S.-Y. Zhu, Phys. Rev. A **76**, 062322 (2007).
[47] T. Yu and J. H. Eberly, Science **323**, 5914 (2009).
[48] B. Bellomo, G. Compagno, A. D'Arrigo, G. Falci, R. Lo Franco, and E. Paladino, Phys. Rev. A **81**, 062309 (2010).
[49] T. J. G. Apollaro *et al.*, New J. Phys. **12**, 083046 (2010).
[50] R. Vasile, S. Olivares, M. G. A. Paris, and S. Maniscalco, Phys. Rev. A **80**, 062324 (2009).
[51] R. Horodecki and M. Horodecki, Phys. Rev. A **54**, 1838 (1996).
[52] J. Medford *et al.*, Nat. Nanotechnol. **8**, 654 (2013).
[53] B. M. Maune *et al.*, Nature (London) **481**, 344 (2012).
[54] J. Cai, G. G. Guerreschi, and H. J. Briegel, Phys. Rev. Lett. **104**, 220502 (2010).
[55] N. Lambert *et al.*, Nat. Phys. **9**, 10 (2013).
[56] N. Lambert, S. D. Liberato, C. Emary, and F. Nori, New J. Phys. **15**, 083024 (2013).
[57] M. Tiersch, G. G. Guerreschi, J. Clausen, and H. J. Briegel, J. Phys. Chem. A **118**, 13 (2014).
[58] V. V. Mihailov, J. Phys. A **10**, 147 (1977).